Corrosion of pipelines used for CO_2 transport in CCS: is it a real problem?

Ivan S. Cole[*,1], Penny Corrigan[1], Samson Sim[1,2] and Nick Birbilis[2]
CSIRO Materials Science and Engineering
Private Bag 33, Clayton South, Victoria 3169, Australia
Department of Materials Engineering, Monash University,
Clayton, Victoria 3800, Australia

ABSTRACT

The transport of carbon dioxide (CO_2) from capture to storage is a vital aspect of any CO_2 capture and storage (CCS) process - and it is essential that it is effective, safe and economical. Transport by pipelines is one of the preferred options and thus, for safe operations, such pipelines should not be subject to internal corrosion. Present CO_2 pipelines used for enhanced oil recovery (EOR) have suffered only minimal corrosion over the last 20 years, however, such pipelines operate under stringent regulations with regard to water and contaminant levels in the CO_2 stream. This paper reviews the literature on the range of potential compositions in CCS CO_2 streams and the likely phases that will be in such streams, the relevant history of CO_2 pipelines, and laboratory studies of CO_2 corrosion, with a view to understanding the corrosion threat to pipelines where CO_2 is the primary fluid.

Keywords: CO_2, corrosion, SO_2, transport, water

---

[*] Corresponding author at: CSIRO Materials Science and Engineering, Private Bag 33, Clayton South, Victoria 3169, Australia.
E-mail address: Ivan.Cole@csiro.au (I. Cole).

1. Introduction

In order to minimise carbon dioxide (CO_2) emissions from power plants and other industrial processes, safe and economical CO_2 capture and storage (CCS) systems are being developed (Carter, 2010; Connell, 2005). Transport from the CO_2 source to the storage location is a key element in all CCS systems, with pipelines being the logical and preferred transportation method. The aim of this review is to ascertain if the literature contains sufficient information to assess whether CCS CO_2 pipelines can be operated without the risk of internal corrosion, and/or to identify any knowledge gaps that need to be filled in order to make such an assessment.

CO_2 pipelines have been extensively used in enhanced oil recovery (EOR) - currently ~3100 miles (~5000 km) of CO_2 pipeline is used principally for EOR in the USA alone - for up to 20 years with no significant record of corrosion (Gale and Davison, 2004). Such pipelines are operated under strict limitations on contaminants, particularly free water, H_2S, S compounds and oxygen (Carter, 2010). In CCS, in order to avoid two-phase flow, CO_2 will be transported either in the supercritical or the liquid state—at pressures ranging from >5 to >10 MPa[†]. At these pressures, the solubility of water is limited ($0.3–0.4 \times 10^{-2}$ mole fraction) (Spycher et al., 2003). If a separate, H_2O rich, aqueous phase forms, it will be saturated with CO_2 and will have an acidic pH of ~3, via speciation of carbonic acid, as shown Fig. 1.

A recent paper by Choi and Nesic gave an excellent description (theoretically and experimentally) of the mutual solubility of water in CO_2 and CO_2 in water; certain aspects of which are reviewed below. However, one key aspect of CCS transport systems, in particular, is that additional contaminants such as H_2S, SO_3 and NO_3 will also segregate to the aqueous phase and thus have the potential to drop the solution pH further, via the in situ formation of sulfuric and nitric acids (in addition to the existing carbonic acid). Experimental work (Ayello et al., 2010) has shown that the presence of a second acidic aqueous phase has the potential to significantly increase the corrosion rate of pipeline steels.

In a water-mediated system, three types of reactions can occur:

[†] 100 Bar = 10MPa

a) The absorption of gaseous CO_2 and the acidification of the moisture layer (Carter, 2010; Connell, 2005; Gale and Davison, 2004).
b) Cathodic (Spycher et al., 2003; Ayello et al., 2010) and anodic (Zhang and Cheng, 2009) reactions.
c) Reactions leading to the formation of an oxide layer (Glezakou et al., 2009; Nešić, 2007; Granite and O'Brien, 2005).

The absorption of CO_2 occurs via:

$$CO_2(g) + H_2O(l) \leftrightarrow H_2CO_3(aq) \quad (1)$$
$$H_2CO_3 \leftrightarrow H^+ + HCO_3^- \quad (2)$$
$$HCO_3^- \leftrightarrow H^+ + CO_3^{2-} \quad (3)$$

In such a regime, cathodic reactions may occur either by the direct reduction of hydrogen ions, or via carbonates:

$$2H^+ + 2e^- \rightarrow H_2 \quad (4)$$
$$H_2CO_3 + e^- \rightarrow HCO_3^- + ½ H_2 \quad (5)$$
$$HCO_3^- \rightarrow CO_3^{2-} + ½ H_2 \quad (6)$$

The anodic reaction occurs simply via the oxidation of iron:

$$Fe \rightarrow Fe^{2+} + 2e^- \quad (7)$$

Oxides may form either via a one-stage reaction with carbonates, or via a two-stage reaction with bicarbonates:

$$Fe^{2+} + CO_3^{2-} \rightarrow FeCO_3 \quad (8)$$
$$Fe^{2+} + 2HCO_3^{-} \rightarrow Fe(HCO_3)_2 \quad (9)$$
$$Fe(HCO_3)_2 \rightarrow FeCO_3 + CO_2 + H_2O \quad (10)$$

Experimental evidence for the presence of carbonate ($FeCO_3$) layers upon steel has been shown in Choi (2010). Iron is known to be very active in acid solution, and this activity may be attributed to the instability of any oxide or carbonate formation, and to the support of the cathodic reaction (Glezakou et al., 2009) induced by the high hydrogen ion concentration. Thus, the acidification of the aqueous phase in CO_2 transport can very significantly increase pipeline corrosion rates. The works to date, experimental and theoretical, indicate that a worst-case scenario can be a pH value of the fluid of ~3.2 (from carbonic acid alone). The impact of this low pH can be predicted to some extent by the Pourbaix diagram for Fe, which reveals the enhanced dissolution of Fe with decreasing pH.

At present, one of the major limitations in CCS is the associated infrastructure and running costs, and thus significant effort is being directed at reducing these costs. Measures being considered include reducing the extent of gas conditioning (i.e. CO_2 drying) prior to gas entering a pipeline, and/or combined gas capture (Carter, 2010), however, both of these measures have the potential to increase the levels of pipeline contaminants, thus increasing the threat to durability.

This review will not focus on the problem of corrosion in CO_2-containing streams in which CO_2 is not the principal phase, such as those that occur in the oil and gas pipeline industry. Although superficially similar to the corrosion problem in CCS, the scenario in oil and gas streams is quite different, in part because the concentrations of CO_2 are different, but also because the pressures are much lower (hence CO_2 is in the gas phase) and the primary fluid is not CO_2. The reader is referred to the review of Nešić (2007) for information on this topic.

2. Effect of capture on contamination in CO_2 streams

In considering the impurities in captured CO_2 that are required to be transported, one needs to appreciate the different mechanisms of separation, and the likely impurities that will result from each method. Technologies currently under consideration for CO_2 capture include absorption, adsorption, membrane and cryogenic processes (Granite and O'Brien, 2005). Of these, the most likely candidate for commercial application in the near future is chemical absorption using solvents (most commonly alkanolamines, particularly monoethanolamine (MEA)) to form weakly bonded intermediate compounds, which are subsequently recovered through the application of heat (Granite and O'Brien, 2005). However a major issue with MEA systems is that the amines react irreversible with sulphur bearing compounds and O_2 (Wolsky et al. , 1994). As detailed later this is determental to the MEA (rendering it inactive) but does also reduce the contaminants (particularly sulphur compounds)in the CO2 gas

Formatted: Subscript

Formatted: Not Superscript/ Subscript stream. This interaction has been observed in MEA CO_2 recovery pilot units attached to power plants (Wilson et al., 1992 , Suda et al. , 1992) while Suda et al.(1992) indicating that 100% of the SO_2 in the input gas stream reacted with the MEA.

Formatted: Subscript

Formatted: Subscript

An analysis by Lee et al. (2009) of the likely impurities in captured CO_2 streams using MEA-based CO_2 absorption, indicated that the initial composition of flue gas from a coal-fired power plant may consist of 500–3000 ppmv of SO_2, 20–30 ppmv of SO_3, and up to 100 ppmv of HCl, in addition to mercury and NO_x (which will consist of 95% nitric acid and 5% NO_2). Many of the components of flue gas (particularly SO_2) may react with MEA, causing its irreversible degeneration with the precipitation of stable salts. This suggests that there are economical benefits to purifying the gas prior to CO_2 absorption, although these must be balanced against the cost of purification.

Fig. 2 shows possible pollutant control measures for a typical coal-fired power plant, which include a low NO_x burner (LNB), selective catalytic reduction (SCR) (to reduce NO_x levels), an electrostatic precipitator (ESP) and flue gas desulfurization (FGD).

In their estimate of contaminant levels in CO_2 streams from a 500 MW coal-fired power plant, Lee et al. (2009) assumed five case scenarios with different control measures, as per Table 1. It is evident that, depending on the pollutant control procedures, the contaminant levels varied dramatically from 0.5 to <0.1%. It is known that if SO_2 enters a CO_2 absorber, it may react with the MEA, leading to the formation of heat-stable salts (isothiocyanatoethane and tetrahydrothiophene), which must be removed from the bottom of the heat exchanger and disposed of. For case 5 in Table 1, which includes MEA-based CO_2 capture, it is assumed that either 0 or 75% of the SO_2 reacts to form such heat-stable salts. While there is some uncertainity about the degree of capture of SO2, 75% seems a reasonable estimate based on the work of Suda et al. (1992) and others previously discussed. The best possible scenario (case 5 with the formation of stable salts) leads to 34 ppmw of SO_2, <21 ppmw of SO_3, <7 ppmw of NO_2, <2 ppmw of HCl and <2 ppbw of Hg^{2+}.

In addition to the cleaning processes outlined above, CO_2 gas streams may undergo conditioning before transport through pipes (Aspelund and Jordal, 2007). Gas conditioning can include the removal of water and other liquids in vapour–liquid separator drums, the use of a volatiles removal column to extract gases such as N_2, O_2, NO, CO, H_2 and CH_4, and additional physical and/or chemical treatments to remove other unwanted components. In liquid–vapour separation drums, water is initially removed using gravity alone, and then additional water is removed using pressures of between 20 and 40 bar. Indeed, Austegrad et al. (2006) indicate that water content can be lowered to 400–500 ppm. This is below the solubility limit of H_2O in liquid or supercritical CO_2, which according to Spycher et al. (2003) is around 3×10^{-3} g/g or approximately 730 ppm.

3. Chemistry (phases and pH) likely in CO_2 streams

For cost-efficient and safe transport, CO_2 needs to be in either the liquid or supercritical state, and so will be at pressures in excess of 50 and 80 MPa, respectively, at temperatures above 0°C. Austegrad et al. (2006) compared a range of thermodynamic models with measured data on $H_2O–CO_2–CH_4$ mixtures, and the models and data on the $H_2O–CO_2$ system are of importance to this review. Fig. 3 shows the phases in such a system in the case where there is free water, and it is evident that water will be in the liquid phase when CO_2 is transported in either the supercritical or liquid state.

However, if the water content is kept low, it will remain dissolved in the CO_2 phase. King et al. (1992) experimentally determined the solubility of water in supercritical and liquid CO_2 at temperatures of 15–40°C and at pressures of 1–200 bar, and found that the mole fraction of water in CO_2 ranged from just over 0.22×10^{-2} at 15°C and 40 bar, to around 0.58×10^{-2} at 40°C and 200 bar. King et al. (1992) also provided an estimation of how much molecular H_2CO_3 may result from the hydration of CO_2 (0.32% of CO_2 concentration). Numerous researchers (Akinfiev and Diamond, 2010; Austegrad et al., 2006; Ayello et al., 2010; Bermejo et al., 2005; Bruusgaard et al., 2010; Chapoy et al., 2004; Fu et al., 2009; Glezakou et al, 2010; Jacquemet et al., 2009; Koglbauer and Wendland, 2008; Kwon et al., 2010; Lachet et al., 2009; Lee et al., 2002; Li and Yan, 2009; Longhi, 2005; Pappa et al., 2009; Song et al., 1987) have since developed models or experimental data for the mutual solubility of water and CO_2, and these have been reviewed by Spycher et al. (2003) and more recently by Choi (2010). Their analyses indicated that the solubility of water goes through a sharp U-type curve (see Fig. 4a for water solubility in CO_2), whereby it decreases sharply as pressure is increased to 50–60 bar, then it increases rapidly before stabilising at 60–80 bar and then on being only a weak function of pressure, with the solubility limit of water increasing from around 0.3×10^{-2} (mole fraction) at 100 bar, to 0.4×10^{-2} at 500 bar. The experimental data and the modelled data reviewed by Spycher et al. (2003) are consistent with each other, with the earlier data of King et al. (1992), and with the later solubility analysis of Austegrad et al. (2006). In addition, the solubility of CO_2 in water is also shown in Fig. 4b. The immediate practical information that is revealed from Fig. 4 is that as temperature decreases, solubility increases, and as pressure increases, solubility also increases.

As suggested above, a CCS CO_2 pipeline is likely to operate at pressures above 80 bar when the solubility of water is relatively constant, however as indicated in Fig. 4, if there is a significant change in pressure, the solubility of water in supercritical or liquid CO_2 can change dramatically. For example, increasing the pressure from 20 to 80 bar at 300 K would drop the solubility of water from 6.37×10^{-3} to 2.02×10^{-3}, and thus an aqueous phase would form (as outlined in Section 2, this phenomenon is used in gas conditioning to lower the water content going into CO_2 pipes). In this case, assuming that H_2O is at the solubility limit at the lower pressure and that the pressure is increased to 80 bar, then the mass of the water phase would be 0.45% and it would consist of 97% H_2O and 3% CO_2. Further, a similar decrease in the solubility of water from 2.7×10^{-3} to 0.9×10^{-3} could occur if the pressure was dropped from 80 bar (at 20°C) to 60 bar. Similar variations could occur with temperature changes. For example, at 300 and 320 K (at 80 bar) the solubility of water in CO_2 would be 2.02 and 4.39×10^{-3}, respectively (Spycher et al., 2003), so that if water was at saturation at the higher temperature and then temperature decreased, the mass of the water phase would be 0.24% (again 97% H_2O and 3% CO_2). Such variations in pressure and/or temperature could occur along a pipeline (see Section 4).

Ayello et al. (2010) examined (both experimentally and using a simulation program by OLI Systems (2010)) phase mixtures of different impurities in pure CO_2 at 75.8 bar at 40°C, and found that up to 2 g of water per kg of CO_2 (i.e. 0.2% by weight) would remain in solution, after which a separate aqueous phase would form. This aqueous phase would have a pH of 3.1, independent of the water concentration. The authors found that while the addition of NaOH did not change the water solubility limit, it could change the pH, i.e. 1 g of NaOH raised pH to 6 for water contents of 2–5 g per kg of CO_2. Likewise, adding HCl to CO_2–H_2O mixtures did not change the water solubility limit, but “high” HCl contents (1g HCl per kg CO_2) dramatically lowered the pH of the aqueous phase (to –4.1). Similar results were found with the addition of HNO_3, with water condensate having a pH of –3.1 when 1g of HNO_3 was added to CO_2–H_2O mixtures.

4. Pressure changes in pipelines and related operational issues

Svensson et al. (2005) have looked at issues related to the transport of CO_2 in CCS, and have highlighted that some EOR pipelines are run at pressures greater than 10 MPa (above the miscibility pressure of CO_2 in oil), however, there can be significant drops in pressure and temperature along a line. Eldevik et al. (2009) also highlight that frictional forces may reduce the pressure in a pipeline during transmission if there is no intermediate compression or large terrain variations, while temperature may be reduced due to heat exchange with the environment. The impact of these changes is highlighted diagrammatically in Fig. 5. Across a pipeline from inlet to outlet (green line in Fig. 5), the factors outlined above could lead to a drop in temperature and pressure, which in turn could lead to a change from a supercritical fluid to a liquid, however the CO_2 would remain in a single phase. The drop in temperature and pressure would, however, reduce the solubility of water in the CO_2 phase and, if the amount of water was close to the solubility limit at the higher temperature and pressure, could lead to the formation of an aqueous phase. Eldevik et al. (2009) also highlighted that if the pipe is depressurised due to pipe failure or a planned operation, then the pressure will drop to the liquid–vapour line and CO_2 vapour will form (blue line in Fig. 5). If the pressure continues to drop, heat will be extracted from either the CO_2 or the ambient to support the phase transformation from liquid to gas, and the conditions will move down the liquid–vapour line. If depressurisation is sufficiently fast, the conditions will reach the triple point where dry ice will form, which can severely hamper the resumption in operations. As the pressure drops, the probability of the formation of an aqueous phase would steadily increase.

5. In-field data

The long-distance transport of CO_2 is now common, with ~3100 miles (~5000 km) of CO_2 pipelines used principally for EOR in the USA alone. Such pipelines operate under strict limitations on contaminants. For example, those adopted by Kinder Morgan (the largest operator of CO_2 pipelines in the USA) require no free water, ≤20 ppm H_2S, ≤35 ppm S compounds, ≤10 ppm O_2, ≤4% nitrogen, ≤5% hydrocarbons (Carter, 2010) and ≤600 ppm H_2O (Connell, 2005). In general, CO_2 pipelines are made from high-strength carbon steels

(X65 to X80), however corrosion-resistant alloys such as 304L are required for certain sections of pipe, such as those upstream of the dehydration unit,

Analysis of corrosion rates in field exposures of CO_2 transport pipelines in the US has shown low corrosion rates (0.00025–0.0025 mm/year), while analysis of CO_2 pipeline incidents in the US from 1990 to 2001 (Gale and Davison, 2004) revealed only 10 incidents (only 2 associated with corrosion), or 0.32 incidents per 1000 km. This compares with 0.17 incidents per 1000 km for natural gas pipelines, and 0.82 incidents per 1000 km for hazardous liquids pipelines.

Some pipelines in North America currently do carry CO_2 gas with contaminants, for example a 325 km pipeline conveys CO_2 with up to 0.9% H_2S from a gasification facility in North Dakota to EOR fields in Saskatchewan, Canada (Carter, 2010). Further, in Alberta, Canada, CO_2 and H_2S are captured at natural gas processing plants, and transported via 20–200 km pipelines to injection sites. Such pipelines have been operating for two decades with no significant incidents (Bachu and Gunter, 2005).

6. Corrosion data

There have been limited studies of corrosion in conditions encountered in the transport of CO_2 in CCS, and these have been undertaken under fairly severe conditions, however Russick et al. (1996) and Wu et al. (2004a) have studied corrosion in supercritical CO_2 (in relation to its role as a solvent). Russick et al. (1996) investigated the corrosion of stainless steel (304L and 316), aluminium (2024, 6061, and 7075), copper (CDA101) and carbon steel (1018) in pure supercritical CO_2, and CO_2 contaminated with water (3%) or methanol (10%). They observed that no corrosion occurred in pure supercritical CO_2, only the carbon steel corroded in water-contaminated CO_2, and the copper and aluminium 2024 samples corroded in methanol-contaminated CO_2. Wu et al. (2004b) used electrochemical impedance spectroscopy (EIS) to study the development of surface films on carbon steel when exposed to water saturated with supercritical CO_2 (60–150°C and 8.274 MPa). They found that the films slowed down the corrosion rate (initially quite significant at 8.6 mm/year at 90°C over the first 24 hours), and that those produced at higher temperatures were more compact and continuous, and thus more protective.

Very recently, Choi and Nesic (2010) performed some exposure tests in an autoclave and suggest that corrosion rates of steel can vary from ~0.2mm/yr to 20mm/yr as the CO_2 goes from high purity to water saturated. Ayello et al. (2010) also studied the corrosion of steel in supercritical CO_2 contaminated with water plus NaOH, methyl diethanolamine (MDEA), HCl and HNO_3—conditions that could pertain to CO_2 transport in CCS, although the contaminant levels were high compared to those reported earlier in this review. While their modelling indicated that 2000ppm of water was required for the formation of an aqueous phase under their testing conditions, they found significant corrosion (1.2 mm/year^{-1}) occurred at 100 ppm of water. The corrosion rate did increase with increased water content, although not dramatically (2.5 mm/year^{-1} at 200 ppm). The authors suggest that the corrosion rate at low water contents may be due to either the presence of residual water on the steel from prior to exposure to the supercritical CO_2, or to crevices on the steel electrode that stabilise the water films. The addition of 1 g of NaOH almost halved the corrosion rate (at 1000 g of water), while the addition of MDEA dramatically reduced the corrosion rate (100 ppm of MDEA with 100 ppm of water resulted in a corrosion rate of 0.1 mm/year^{-1}). In contrast, the addition of HCl and HNO_3 dramatically increased the corrosion rate. For example, 3.6×10^{-5} g of HCl per kg of CO_2 (and 1000 ppm water) increased the corrosion rate to 5.6 mm/year^{-1} (from 2.3 for the equivalent CO_2–H_2O mixture), while 6.3×10^{-5} g of HNO_3 in the same mixture increased the corrosion rate to 4.5 mm/year^{-1}. The phase analysis and the corrosion rates indicate that the contaminants in CO_2–H_2O mixtures segregate to the aqueous phase, and can dramatically change both the pH of this phase and the corrosion rate induced by it.

McGrail et al. (2009) looked at the corrosion of steel in liquid CO_2, both with and without a separate water phase, and initial experiments revealed rapid corrosion when liquid CO_2 (7 MPa, 25°C) was saturated with water. More controlled corrosion experiments at 998 and 610 ppmw of H_2O resulted in visible corrosion of steel after 21 days in the first environment, but no corrosion after 42 days in the latter, which suggests that there is a threshold water content limit at ~600 ppm, above which corrosion will be induced. At this pressure, water solubility is 1100 ppmw in CO_2 and thus corrosion would occur in the absence of a separate aqueous phase. McGrail et al. (2009) found that the addition of H_2S (321 ppmw) appeared to generate corrosion at a water content lower (408 ppmw) than the limit indicated above, however they argue, through reference to molecular simulation work, that CO_2 absorption and cleavage from Fe surfaces may play a role in inducing corrosion.

Choi et al. (2010) found that the corrosion rate of carbon steel (API 5L X65) in water-saturated CO_2 at 80 bar was 0.38 mm/year. Experiments with the addition of O_2 at partial pressures of 1.6, 3.3 and 5.1 bar (2, 4 and 6%), resulted in a maximum corrosion rate of 1 mm/year at the partial pressure of 3.3 bar. The addition of 0.8 bar SO_2 increased the corrosion rate to 5.6 mm/year, while the addition of 0.8 bar SO_2 plus 3.3 bar O_2 increased the corrosion rate to 7 mm/year. Interestingly, a 13Cr steel exposed to the latter test solution also corroded at 7 mm/year. However, no corrosion was observed in the CO_2–SO_2–O_2 mixture without the presence of water. Examination of corroded specimens indicated that a thick $FeCO_3$ layer had formed in the water-saturated CO_2 test, while a porous iron oxide layer formed if oxygen was added. The corrosion product in the SO_2-containing mixtures was $FeSO_3.3H_2O$. The work of Choi et al. (2010) highlights the importance of O_2, which may simultaneously provide an additional cathodic reaction pathway and inhibit the formation of a protective iron-carbonate layer. Parallel work by Singer et al. (2007) on the corrosion of carbon steels in oil and gas applications indicates that a small amount of H_2S in the presence of CO_2 may, in fact, significantly reduce the corrosion rate by promoting the formation of a stable and compact mackinawite film.

7. General discussion

To assess the possibility of corrosion during the transport of CO_2 in CCS, it is useful to classify the likely conditions that may prevail in a pipeline into four different regimes:
A — Very low contaminant levels and extremely low water content.
B — Low contaminant levels and water content below the solubility content.
C — Low contaminant levels and water content above the solubility content.
D — Moderate contaminant levels and water content above the solubility limit.

The first regime currently relates to CO_2 transport in EOR in the USA (under Kinder Morgan guidelines) and would prevail if CO_2 were extracted using MEA in a plant with FGD and LNB/SCR, followed by gas conditioning to lower the water content below the pressure solubility limit (500 ppm). The second regime would occur if gas conditioning was limited or there was a limited source of H_2O into the pipe. The third could occur in the absence of gas conditioning, or with gas conditioning and significant changes to pipe conditions (lowering pressure and temperature), and/or an additional source of H_2O. The last condition would occur if contaminant removal was limited at a power plant or if, for economic reasons, contaminant gases were transported along with the CO_2.

Regime A—Both established experience with CO_2 pipelines and laboratory work indicate that very low corrosion rates occur if both H_2O and other contaminants are tightly controlled. The laboratory studies of McGrail et al. (2009) indicate that ~600 ppmw is the critical value for water content to induce significant corrosion. This is in contrast to the work of Ayello et al. (2010) who found significant corrosion at 100 ppmw, although they did indicate that residual water may have contributed to this corrosion rate. The experimental value of 600 ppmw water content derived by McGrail et al. (2009) matches the EOR CO_2 transport limit of 600 ppm. Thus, although there is some concurrence for a critical value of 600 ppm of H_2O in CO_2 (below which no significant corrosion occurs), the exact value of this limit needs to be confirmed.

Regime B—Laboratory studies (Ayello et al., 2010; Russick et al., 1996; Choi et al., 2009) indicate that significant corrosion can occur when the H_2O level exceeds a critical value, even in the absence of an aqueous phase. In the absence of additional contaminants, Choi et al. (2009) found a corrosion rate of 0.38 mm/year for water-saturated CO_2, while Ayello et al. (2009) found a corrosion rate of 2.5 mm/year^{-1} at a water content of 200 ppm (O_2 level not measured). The work of Choi et al. (2009) indicates that the corrosion rate will increase as the level of other contaminants also increases, however, the levels of these contaminants (e.g. 2–6% of O_2) are much higher than the limits imposed for EOR CO_2 transport (10 ppm of O_2 or 35 ppm of S compounds) or the SO_2 limit that would arise by applying MEA capture to a clean power plant (34 ppmw) (Lee et al., 2009). Thus, two questions remain unresolved: What are the likely corrosion rates in liquid or supercritical CO_2 with H_2O concentrations below the solubility limit but above the critical limit? What is the effect of low levels of additional pollutants on these contaminants?

Regime C—Laboratory studies indicate that corrosion rate can increase dramatically if the H_2O content passes the solubility limit and an aqueous phase forms, particularly if other contaminants are present. As indicated earlier, Ayello et al. (2010) found that the addition of small amounts of HNO_3 and HCl to 1000 ppm of water in supercritical CO_2 increased corrosion rates to 4.5 and 5.6 mm/year^{-1}, respectively. In fact, Ayello et al. (2010) added 36 ppb of HCl and 63 ppb of HNO_3, which are significantly below the HCl and NO_x contamination levels outlined by Lee et al. (2009) for MEA-captured CO_2 from a clean coal-fired power plant. The high corrosion rates can be explained in part by HNO_3 and HCl segregating to the aqueous phase and dramatically lowering the pH of that phase, thus increasing the corrosion rate of steel. For a given concentration of additional contaminant (e.g. HNO_3 or HCl), the pH of the aqueous phase will decrease as the percentage concentration of the aqueous phase increases, and thus it is unclear if the corrosion rate will fall or rise as the water content increases above the solubility limit.

Regime D—As yet, there are no direct records of corrosion rates under this regime, however the work of Choi et al. (2010) revealed high corrosion rates (up to 7 mm/year^{-1}) with H_2O-saturated CO_2 and high SO_2–O_2 levels (SO_2 levels tested were of the same order as those predicted by Lee et al. (2009) for CO_2 streams prior to MEA capture in the absence of FGD.

Significant corrosion is likely to occur under regimes B–D, and under regimes C and D it would certainly be at such levels to necessitate intervention, either by the application of a coating technology, the use of a cathodic protection system, or by a program of monitoring and repair. At present, the corrosion rate expected under regime B is not clear, with more experimental work required to resolve the significant differences between the two current studies. The exact regime applicable to CO_2 transport in CCS will depend very much on the capture, gas cleaning and sequestration strategies in place. If a comprehensive range of pollutant control measures were adopted at a plant, combined with MEA-based capture and gas conditioning, then the CO_2 would be very low in contaminant levels (i.e. regime A). However, if for economic reasons a less rigorous strategy is adopted, then the pipeline may fall into regimes B, C or D, and additional corrosion prevention measures would be required.

Experimental data indicates that if the H_2O content is above 600 ppm but below the solubility limit so there is no separate aqueous phase, then significant corrosion can occur. The experimental data is supported by the modelling work of Glezabou et al. (2009), which also indicates that a protective iron carbonate layer may form that will slow the corrosion rate, but that this layer can be replaced by iron oxides if significant oxygen is present. However, this mechanism should occur even in the absence of water, and so cannot explain the apparent existence of a critical water content. More recent work by Glezabou et al. (2010) explores corrosion mechanisms in the absence of an aqueous phase, using density functional theory and periodic slab models to show that CO_2 is spontaneously activated in the presence of a clean Fe(100) surface. In this process, there is a charge transfer from the surface to the CO_2 moiety. The absorbed CO_2 may then dissociate and react with other CO_2 molecules, forming CO_3^{2-} on the surface. Interestingly the formation of H_2CO_3 is unlikely. Thus, Glezabou et al. (2009; 2010) indicate that corrosion can occur in the presence of only CO_2, and that the formation of an iron carbonate layer would be expected. Notwithstanding this work, currently the corrosion community's understanding of corrosion in non-aqueous fluids is very limited, and more in-depth studies are required to examine the competitive or perhaps synergistic interactions between H_2O, CO_2 and other contaminants, and Fe surface processes.

Experimental work indicates that high corrosion rates may result if an aqueous phase exists, particularly in the presence of contaminants that may acidify this aqueous phase. However, such tests have been carried out in laboratory chambers and cannot account for flow effects in pipelines. The aqueous phase will have a lower density than the CO_2 phase, which may have an influence on both its transport and its agglomeration. In most system the aqueous phase will be small (typically <1%, see Section 2). Corrosion would occur when the aqueous phase comes into contact with a pipe wall, however if the aqueous phase is well dispersed in the majority fluid, then any given section of the pipe should only infrequently come into contact with the aqueous phase. However, if a mixed flow pattern leads to agglomeration of the aqueous phase or preferential flow in certain regions of the pipe, then the frequency of aqueous phase contact with particular parts of the pipe could be dramatically increased.

There are a number of pertinent issues concerning the corrosion rates of steel pipelines that need to be resolved experimentally. These include:

a) The highest concentration of dissolved H_2O in liquid or supercritical CO_2 before appreciable corrosion occurs.
b) The corrosion rate that occurs when the water content in the CO_2 phase excludes the critical value (point 1), but is less than the solubility limit, and the effect of additional contaminants on this corrosion rate.
c) The variation of corrosion rate as water content is increased past the solubility limit (given low but realistic levels of additional contaminants).

The literature raises two intriguing questions for corrosion scientists:

a) What are the mechanisms of corrosion when CO_2 is the fluid, and what roles do dissolved species play in these mechanisms? In particular, if chlorides are present in the contaminant water, will this tend to localise corrosion and be an even more significant corrosion threat.
b) Similarly, what are the corrosion mechanisms when water exists as an isolated phase in CO_2 fluid, and how would the dynamics of pipeline transport influence these mechanisms?

In regards to the above, one can see the impact visually by the calculated diagram that reveals the solubility of phases in water containing CO_2 containing S impurities (i.e. SO_4^{2-}). It is seen that sulphuric acid can exist in appreciable quantities at acidic pH, and as such, the electrolyte pH can decrease significantly below the value of ~3.2 which is a minimum - to values as low as 1. Such similar diagrams could also reveal that nitric/nitrous acid can perform a similar pH decreasing role via N-impurities.

As indicated previously, laboratory data on corrosion rates under conditions likely to occur in CO_2 transport is limited. This is in part because the equipment required to generate high pressures is expensive and therefore only available in a few institutions. However, modelling studies indicate that if an aqueous phase is present then contaminants will preferentially segregate to the aqueous phase, and it is this highly acidic phase that will be corrosive rather than the CO_2 phase that surrounds it. This knowledge should enable the development of test methods that are able to reproduce the most corrosive features of high pressure mixtures, such as CO_2–H_2O–SO_2, without the use of high pressures (e.g. cyclic exposure to highly acidic aqueous solutions, followed by immersion in de-aerated CO_2-rich solutions). The validity of such methods would, of course, need to be demonstrated.

10. Conclusions

A review of the literature on the corrosion of pipelines used for the transport of CO_2 in CCS indicates that:

a) If conditions in a pipeline are maintained so that the water content and other contaminant levels are kept extremely low (i.e. from drying), as is currently the case for EOR pipelines, then corrosion rates are also likely to be sufficiently low, as suggested by empirical evidence. This may occur through a combination of cleaning technologies prior to CO_2 capture , the effect of capture itself (particularly MEA reaction with sulphur compounds and O_2) and post capture gas treatment. However additional research is required to fully quantify the residual contaminates that may enter the CO_2 stram to be transported.

Formatted: Subscript

Formatted: Subscript

Formatted: Subscript

b) From a corrosion perspective, iron is highly active in the acidic pH range. The combination of water with CO_2 leads to the in situ formation of carbonic acid, which even at low concentrations causes a major decrease in the pH of the aqueous phase.

c) The majority of typical impurities—which arise as a result of the nature of the CO_2 source and are hence unavoidable—include S- and N-bearing compounds, which are unfortunately detrimental and lead to the in situ formation of nitric and sulfuric acids in the presence of acidified water. This increases the total acid concentration, lowering pH further (dramatically), and in turn enhancing corrosion rates.

d) It would appear that the principal influence on corrosion rate is the presence of water, since the acidification of water by the CO_2 itself, and any contaminants, is readily possible. The lack of an aqueous phase will minimise corrosion, but there is some evidence that corrosion may still occur even when the water content is below a critical threshold. Further research is needed into corrosion under water-free conditions.

e) In all, experimental testing under conditions that directly relate to CCS is very limited, and significantly more experimental work is required in order to define the fundamental corrosion mechanisms at play. Such testing is not trivial, given the pressures and experimental considerations involved, however there is an urgent and critical need to benchmark corrosion levels, such that estimates of service life can be ascertained. This includes testing over a wide range of variables, since if the corrosion mechanism is highly localised, the potential risk increases accordingly.

Acknowledgements

Samson Sim is supported by an MGS scholarship

References

Akinfiev, N.N., Diamond, L.W., 2010. Thermodynamic model of aqueous CO_2–H_2O–NaCl solutions from –22 to 100 °C and from 0.1 to 100 MPa. Fluid Phase Equilib. 295, 104–124.

Aspelund, A., Jordal, K., 2007. Gas conditioning—the interface between CO_2 capture and transport. Int. J. Greenhouse Gas Control 1, 343–354.

Austegard, A., Solbraa, E., De Koeijer, G., Mølnvik, M.J., 2006. Thermodynamic models for calculating mutual solubilities in H_2O–CO_2–CH_4 mixtures. Chem. Eng. Res. Des. 84, 781–794.

Ayello, F., Sridhar, N., Evans, K., Thodla, R., 2010. Effect of liquid impurities on corrosion of carbon steel in supercritical CO_2. In: Proceedings of the 8th International Pipeline Conference (IPC2010), September 27–October 1, Calgary, Alberta, Canada.

Bachu, S., Gunter, W.D., 2005. Overview of acid-gas injection process in Western Canada. In: Wilson, M., Gale, J., Rubin, E.S., Keith, D.W., Gilboy, C.F., Morris, T., Thambimuthu, K. (Eds.), Proceedings of the 7th International Conference on Greenhouse Gas Control Technologies, September 5–9, Vancouver, Canada. Elsevier, pp. 443–448.

Bermejo, M.D., Martin, A., Florusse, L.J., Peters, C.J., Cocero, M.J., 2005. The influence of Na_2SO_4 on the CO_2 solubility in water at high pressure. Fluid Phase Equilib. 238, 220–228.

Bruusgaard, H., Beltran, J.G., Servio, P., 2010. Solubility measurements for the CH_4 + CO_2 + H_2O system under hydrate–liquid–vapor equilibrium. Fluid Phase Equilib. 296, 106–109.

Carter, L.D., 2010. Capture and Storage of CO_2 and Other Air Pollutants. Report CCC/162, IEA Clean Coal Centre, London.

Chapoy, A., Mohammadi, A.H., Chareton, A., Tohidi, B., Richon, D., 2004. Measurement and modeling of gas solubility and literature review of the properties for the carbon dioxide–water system. Ind. Eng. Chem. Res. 43, 1794–1802.

Choi, Y., Nesic, S., Young, D., 2010. Effect of impurities on the corrosion behavior of CO_2 transmission pipeline steel in supercritical CO_2–water environments. Environ. Sci. Technol. 44, 9233–9238.

Choi, Y., Nesic, S., 2010. Determining the corrosie potential of CO2 transport pipeline in high pCO2-water environments. Int. J. Greenhouse Gas Control (2010). doi:10.1016/j.jiggc.2010.11.008

Connell, D.P., 2005. Carbon Dioxide Capture Options for Large Point Sources in the Mid-Western United States: An Assesssment of Candidate Technologies. Final report. CONSOL Energy Inc., South Park, PA,.

Eldevik, F., Graver, B., Torbergsen, L.E., Saugerud, O.T., 2009. Development of a guideline for safe, reliable and cost efficient transmission of CO_2 in pipelines. Energy Procedia 5, 1579–1585.

Fu, D., Liu, J.M., Yang, Z.A., 2009. Phase equilibria and vapor–liquid–liquid triple point for mixture of CO_2 and water. Acta Chim. Sin. 67, 2662–2668.

Gale, J., Davison, J., 2004. Transmission of CO_2—safety and economic considerations. Energy 29, 1319–1328.

Glezakou, V.A., Dang, L.X., McGrail, B.P., 2009. Spontaneous activation of CO_2 and possible corrosion pathways on the low-index iron surface Fe(100). J. Phys. Chem. C 113, 3691–3696.

Glezakou, V.A., Rousseau, R., Dang, L.X., McGrail, B.P., 2010. Structure, dynamics and vibrational spectrum of supercritical CO_2/H_2O mixtures from *ab initio* molecular dynamics as a function of watercluster formation. Phys. Chem. Chem. Phys. 12, 8759–8771.

Granite, E.J., O'Brien, T., 2005. Review of novel methods for carbon dioxide separation from flue and fuel gases. Fuel Process. Technol. 86, 1423–1434.

Hydra-Medusa software: http://www.kemi.kth.se/medusa/ (accessed February 2011)

Jacquemet, N., Le Gallo, Y., Estublier, A., Lachet, V., von Dalwigk, I., Yan, J., Azaroual, M., Audigane, P., 2009. CO_2 streams containing associated components—a review of the thermodynamic and geochemical properties and assessment of some reactive transport codes. Energy Procedia 1, 3739–3746.

King, M.B., Mubarak, A., Kim, J.D., Bott, T.R., 1992. The mutual solubilities of water with supercritical and liquid carbon dioxides. J. Supercrit. Fluids 5, 296–302.

Koglbauer, G., Wendland, M., 2008. Water vapor concentration enhancement in compressed humid nitrogen, argon, and carbon dioxide measured by Fourier transform infrared spectroscopy. J. Chem. Eng. Data 53, 77–82.

Kwon, C.H., Lee, C.H., Kang, J.W., 2010. Calculation of phase equilibrium for water plus carbon dioxide system using nonrandom lattice fluid equation of state. Korean J. Chem. Eng. 27, 278–283.

Lachet, V., de Bruin, T., Ungerer, P., Coquelet, C., Valtz, A., Hasanov, V., Lockwood, F., Richon, D., 2009. Thermodynamic behavior of the $CO_2 + SO_2$ mixture: experimental and Monte Carlo simulation studies. Energy Procedia 1, 1641–1647.

Lee, K.M., Lee, H., Lee, J., Kang, J.M., 2002. CO_2 hydrate behavior in the deep ocean sediments; phase equilibrium, formation kinetics, and solubility. Geophys. Res. Lett. 29, 2034, doi:10.1029/2002GL015069.

Lee, J.Y., Keener, T.C., Yang, Y.J., 2009. Potential flue gas impurities in carbon dioxide streams separated from coal-fired power plants. J. Air & Waste Manage. Assoc. 59(6), 725–732.

Li, H., Yan, J., 2009. Impacts of equations of state (EOS) and impurities on the volume calculation of CO_2 mixtures in the applications of CO_2 capture and storage (CCS) processes. Appl. Energy 86, 2760–2770.

Longhi, J., 2005. Phase equilibria in the system CO_2–H_2O. I: New equilibrium relations at low temperatures. Geochim. Cosmochim. Acta 69, 529–539.

McGrail, B.P., Schaef, H.T., Glezakou, V.A., Dang, L.X., Owen, A.T., 2009. Water reactivity in the liquid and supercritical CO_2 phase: has half the story been neglected? Energy Procedia 1, 3415–3419.

Nešić, S., 2007. Key issues related to modelling of internal corrosion of oil and gas pipelines—a review. Corros. Sci. 49, 4308–4338.

OLI Systems Software: Morris Plains, NJ. USA. 2010.

Pappa, G.D., Perakis, C., Tsimpanogiannis, I.N., Voutsas, E.C., 2009. Thermodynamic modeling of the vapor–liquid equilibrium of the CO_2/H_2O mixture. Fluid Phase Equilib. 284, 56–63.

Russick, E.M., Poulter, G.A., Adkins C.L.J., Sorensen, N.R., 1996. Corrosive effects of supercritical carbon dioxide and cosolvents on metals. J. Supercrit. Fluids 9, 43–50.

Singer, M., Brown, B., Camacho, A., Nesic, S., 2007. Combined effect of CO2, H2S and acetic acid on bottom of the line corrosion. Proceedings of the NACE Corrosion Conference and Expo, March 11-15, 2007, Nashville, Tennessee, USA. Paper 07661.

Song, K.Y., Rice, U., Kobayashi, R., 1987. Water content of CO_2 in equilibrium with liquid water and/or hydrates. SPE Form. Eval. 2, 500–508.

Spycher, N., Pruess, K., Ennis-King, J., 2003. CO_2–H_2O mixtures in the geological sequestration of CO_2. I. Assessment and calculation of mutual solubilities from 12 to 100°C and up to 600 bar. Geochim. Cosmochim. Acta 67, 3015–3031.

Svensson, R., Odenberger, M., Johnsson, F., Strömberg, L., 2005. Transportation infrastructure for CSS—experiences and expected development. In: Wilson, M., Gale, J., Rubin, E.S., Keith, D.W., Gilboy, C.F., Morris, T., Thambimuthu, K. (Eds.), Proceedings of

Formatted: Justified

the 7th International Conference on Greenhouse Gas Control Technologies, September 5–9, Vancouver, Canada. Elsevier, pp. 2531–2534.

Suda, T., Fujii, M., Yoshida, K., Iijima, M., Seto, T., Mitsuoka, S.1992, Development of flue gas carbon dioxide recovery technology , Energy Convers. Mgnt., 33, pp. 317-324,

Wilson, M.A., Wrubleski, R.M. and Yarborough, L, 1992, Recovery of CO2 from power plant flue gases using amines, Energy Convers. Mgmt., 33, pp. 325-331,

Wolsky, A. M.,Daniels, E. J.,Jody, B. J., 1994, CO_2 Capture from the flue-gas of Conventional fossill-fuel fired power-plants , Environmental Progress. 13(3), 214-219

Wu, S.L., Cui, Z.D., He, F., Bai, Z.Q., Zhu, S.L., Yang, X.J., 2004a. Characterization of the surface film formed from carbon dioxide corrosion on N80 steel. Mat. Lett. 58, 1076–1081.

Wu, S.L., Cui, Z.D., Zhao, G.X., Yan, M.L., Zhu, S.L., Yang, X.J., 2004b. EIS study of the surface film on the surface of carbon steel from supercritical carbon dioxide corrosion. Appl. Surface Sci. 228, 17–25.

Zhang, G.A., Cheng, Y.F., 2009. On the fundamentals of electrochemical corrosion of X65 steel in CO_2-containing formation water in the presence of acetic acid in petroleum production. Corros. Sci. 51, 87–94.

Formatted: Font: 12 pt, Font color: Auto

Formatted: Don't adjust space between Latin and Asian text, Don't adjust space between Asian text and numbers

Formatted: Font color: Auto

Formatted: Font: 12 pt, Font color: Auto

Formatted: Font color: Auto

Formatted: Font: 12 pt, Font color: Auto

Formatted: Font: 12 pt, Font color: Auto

Formatted: Font color: Auto

Formatted: Font color: Auto

Formatted: Font: 12 pt, Font color: Auto

Formatted: Font color: Auto

Formatted: Font: 12 pt, Font color: Auto

Formatted: Font color: Auto

Formatted: Font: 12 pt, Font color: Auto

Formatted: Font color: Auto

Formatted: Font: 12 pt, Font color: Auto

Formatted: Font color: Auto

Formatted: Font color: Auto

Formatted: Font: 12 pt, Font color: Auto

Formatted: Font: 12 pt, Not Italic, Font color: Auto

Formatted: Font: (Default) Times New Roman, 12 pt, Not Italic, Font color: Auto

Formatted ...

Formatted ...

Formatted ...

Formatted ...

Formatted ...

Formatted ...

Formatted ...

Formatted ...

Formatted ...

Formatted ...

Formatted: Line spacing: 1.5 lines

Formatted ...

Formatted ...

Formatted ...

Formatted ...

Table 1. Estimated contaminant levels in captured CO_2 stream from a 500 MW coal-fired power station, depending on level of contaminant control (adapted from Lee et al. (2009))

Case	Description	Contaminant levels
1	No contaminant control	SO_2 0.6–4.4 wt%, SO_3 42–579 ppmv, NO_2 24–111 ppm, HCl 36–835 ppmv, Hg^{2+} 23–261 ppmv
2	SO_2 control by a wet FGD scrubber	SO_2 337–2403 ppmv, SO_3 21–302 ppmv, NO_2 18–87 ppm, HCl 2–44 ppmv, Hg^{2+} 2–27 ppmv
3	NO_x control by LNB/SCR	SO_2 0.6–4 4 wt%, SO_3 42–579 ppmv, NO_2 10–44 ppm, HCl 36–835 ppmv, Hg^{2+} 23–261 ppmv
4	NO_x control by LNB/SCR plus SO_2 control by a wet FGD scrubber	SO_2 337–2403 ppmv, SO_3 21–302 ppmv, NO_2 7–35 ppm, HCl 2–44 ppmv, Hg^{2+} 2–27 ppmv
5	As in Case 4, but also assuming that a commercial MEA-based CO_2 control unit is used to trap CO_2	SO_2 34–135 ppmw, SO_3 <21–<302 ppmw, NO_2 <7–<35 ppmw, HCl <2–<44 ppmw, Hg^{2+} <2–<27 ppbw

Figure captions

Figure 1. The concentration (in log M) of various species for a hypothetical water + CO_2 mixture showing carbonic acid in existence at acidic pH. Diagram was calculated using Hydra-Medusa with a pressure of 100bar at 37C.

Figure 2. Possible pollutant control measures for a coal-fired power plant (adapted from Lee et al. (2009)).

Figure 3. Phases in the CO_2–H_2O system with free water. V= vapour, L= Liquid, H=hydrate, I = ice. The points are actual measurements from different sources (Austegard et al. ((2006)).

Figure 4. Calculated solubility of (a) water in CO_2 (mole fraction) and (b) CO_2 in water (mole fraction) as a function of pressure and temperature (from Choi and Nesic. (2010))

Figure 5. Impact of operational conditions on pressure and temperature in CO_2 pipelines (adapted from Eldevik et al. (2009)).

Figure 6. The concentration (in log M) of various species for a hypothetical water + CO_2 mixture containing SO_4^{2-} impurities. Diagram was calculated using Hydra-Medusa with a pressure of 100bar at 37C.

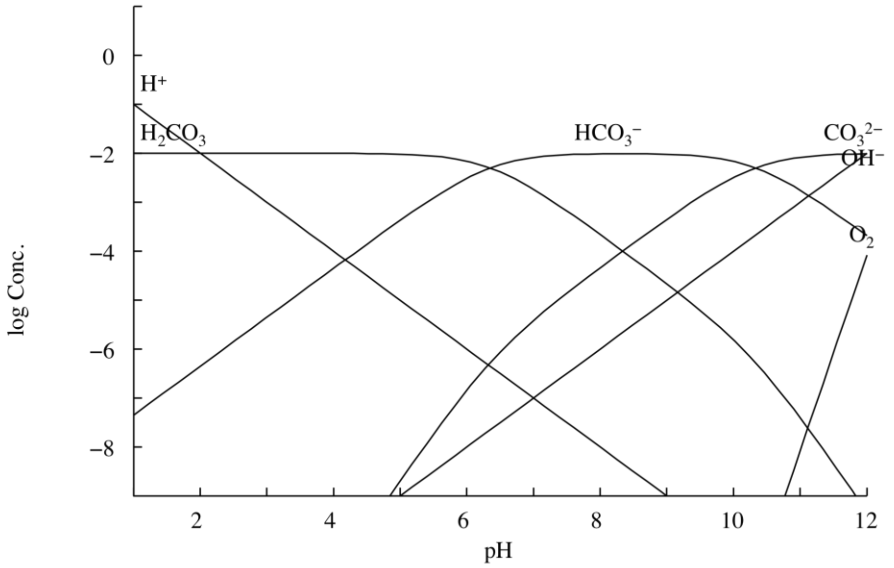

Figure 1. The concentration (in log M) of various species for a hypothetical water + CO_2 mixture showing carbonic acid in existence at acidic pH. Diagram was calculated using Hydra-Medusa with a pressure of 100bar at 37C.

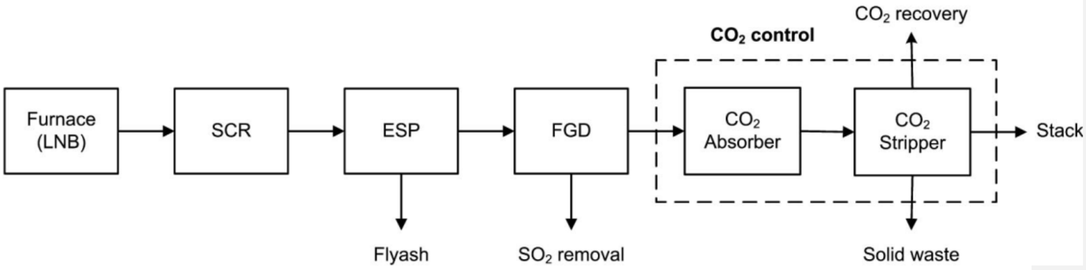

Figure 2. Possible pollutant control measures for a coal-fired power plant (adapted from Lee et al. (2009)).

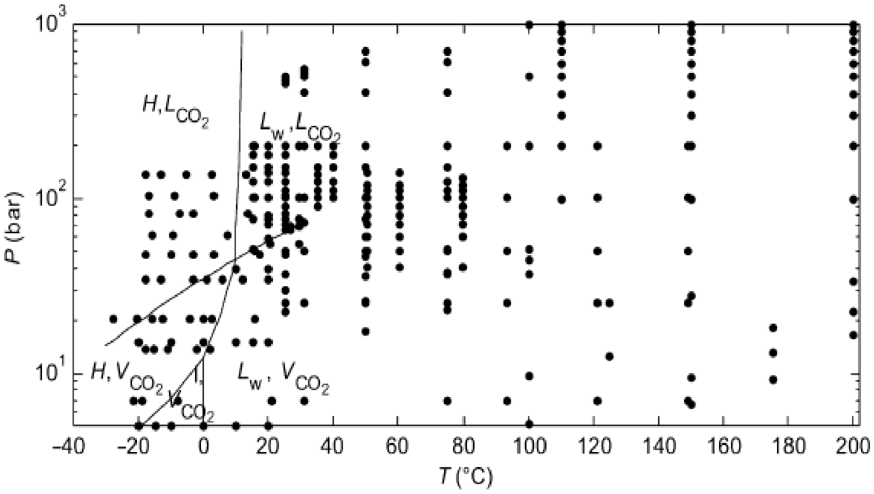

Figure 3. Phases in the CO_2–H_2O system with free water. V= vapour, L= Liquid, H=hydrate, I = ice. The points are actual measurements from different sources (Austegard et al. ((2006)).

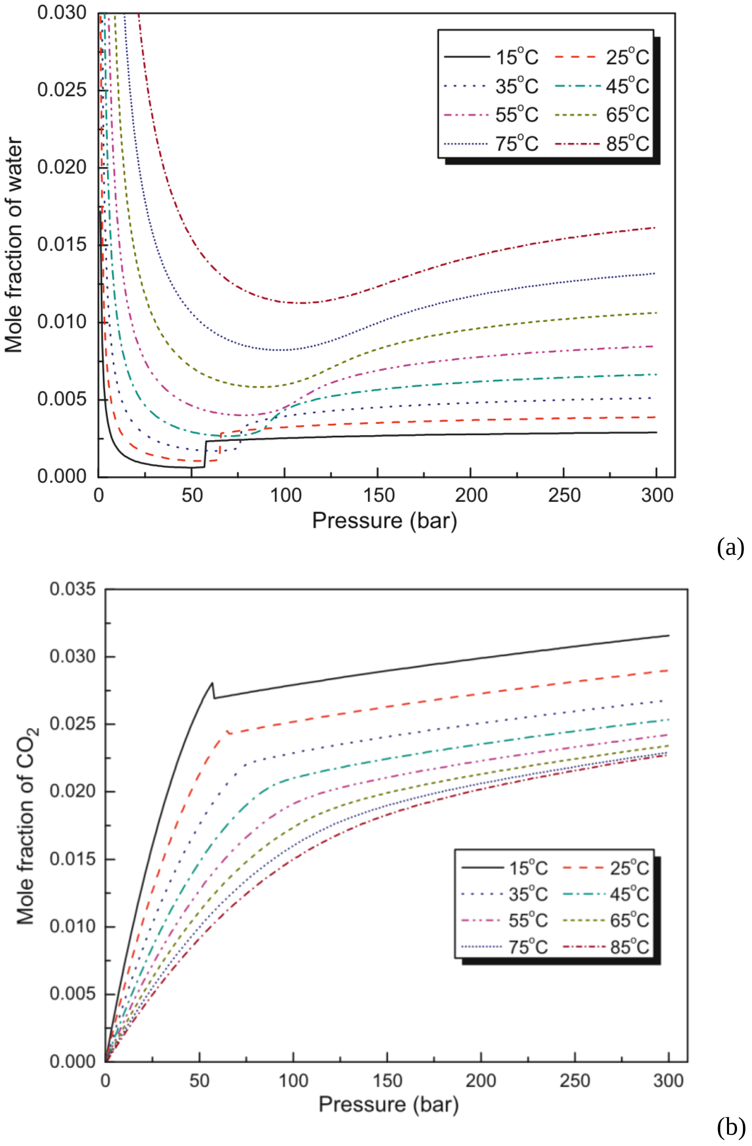

Figure 4. Calculated solubility of (a) water in CO_2 (mole fraction) and (b) CO_2 in water (mole fraction) as a function of pressure and temperature (from Choi and Nesic. (2010))

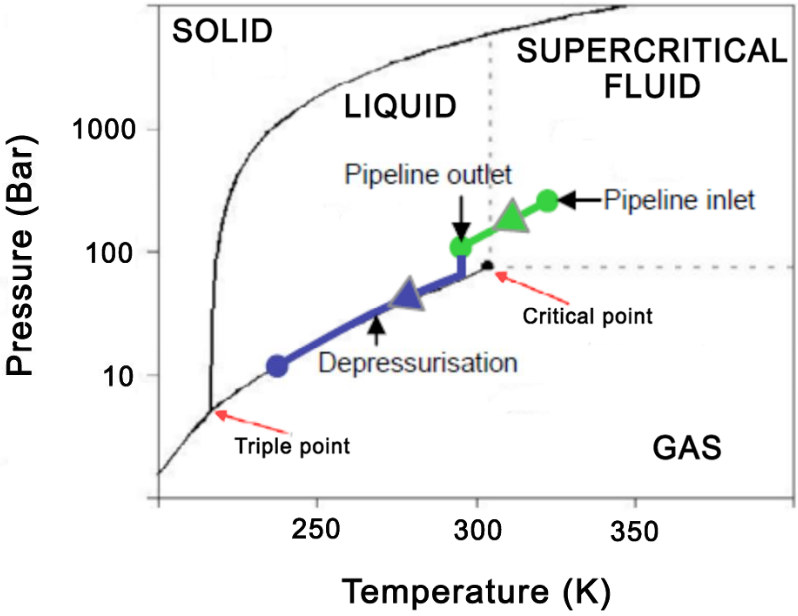

Figure 5. Impact of operational conditions on pressure and temperature in CO_2 pipelines (adapted from Eldevik et al. (2009)).

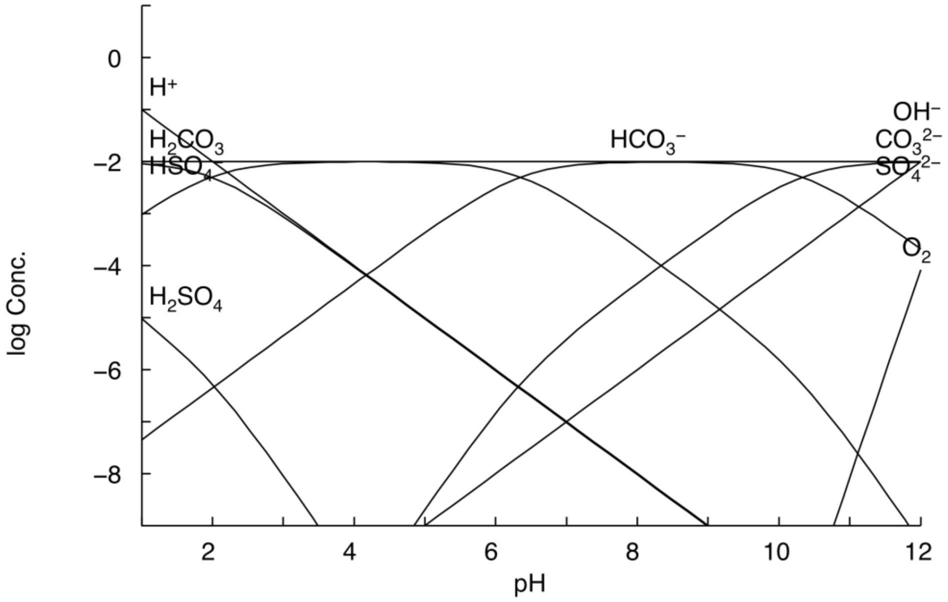

Figure 6. The concentration (in log M) of various species for a hypothetical water + CO_2 mixture containing SO_4^{2-} impurities. Diagram was calculated using Hydra-Medusa with a pressure of 100bar at 37C.